How to cite: *Angew. Chem. Int. Ed.* **2022**, *61*, e202111021
International Edition: doi.org/10.1002/anie.202111021
German Edition: doi.org/10.1002/ange.202111021

Electrochemistry **Hot Paper**

Direct Evidence of Subsurface Oxygen Formation in Oxide-Derived Cu by X-ray Photoelectron Spectroscopy

Hsin-Yi Wang[+], Markus Soldemo[+], David Degerman, Patrick Lömker, Christoph Schlueter, Anders Nilsson, and Peter Amann*

Abstract: *Subsurface oxygen has been proposed to be crucial in oxide-derived copper (OD-Cu) electrocatalysts for enhancing the binding of CO intermediates during CO_2 reduction reaction (CO_2RR). However, the presence of such oxygen species under reductive conditions still remains debated. In this work, the existence of subsurface oxygen is validated by grazing incident hard X-ray photoelectron spectroscopy, where OD-Cu was prepared by reduction of Cu oxide with H_2 without exposing to air. The results suggest two types of subsurface oxygen embedded between the fully reduced metallic surface and the Cu_2O buried beneath: (i) oxygen staying at lattice defects and/or vacancies in the surface-most region and (ii) interstitial oxygen intercalated in metal structure. This study adds convincing support to the presence of subsurface oxygen in OD-Cu, which previously has been suggested to play an important role to mitigate the σ-repulsion of Cu for CO intermediates in CO_2RR.*

Introduction

Transforming CO_2 into value-added fuels and chemicals by means of electrocatalytic conversion, known as CO_2 reduction reaction (CO_2RR), is an attractive approach to alleviate the global imbalance of greenhouse emissions and facilitate energy security.[1] Among various catalysts that have been studied for CO_2RR, copper (Cu) is the only pure metal capable to reduce CO_2 into higher-order hydrocarbons and oxygenates beyond the two-electron transfer products (e.g., formic acid or CO) in comparison to what have been observed on most other metals.[2] It is noteworthy that the activity and selectivity toward multi-carbon products of CO_2RR can be greatly enhanced by fabricating a modified Cu through first oxidizing and subsequently reducing a pristine Cu substrate.[3] The origin of such improved performance on oxide-derived Cu (OD-Cu) has been correlated to several observations. For instance, the nano-structured electrode surface resulted from OD-Cu preparation procedure could increase the local pH in electrolyte, which theoretically alters CO_2RR kinetics.[4] The presence of extended grain boundaries of OD-Cu has been linked to the additional active sites emerging on the surface.[5] It has further been proposed that the non-fully reduced electrode with possible Cu oxide species remaining on its surface could affect the reaction mechanism.[6] In addition, some experimental results lead to the suggestion that either a residual oxide or subsurface oxygen is retained inside OD-Cu under the reducing conditions, and those embedded oxygen species could promote H_2O chemisorption[7] or influence the binding strength of the key CO intermediates.[8] Even though the functionality and stability of subsurface oxygen has been investigated with density functional theory (DFT) using disordered oxide-derived Cu surface model[8b,c] and quasi in situ spectroscopic experiments,[9] respectively, the authenticity of such oxygen species is still debated.[10] A recent isotope labeling experiment[11] analyzed with ex-situ secondary-ion mass spectroscopy (SIMS) concluded that under CO_2RR condition, the concentration of subsurface oxygen present in Cu should be neglectable. The detectable oxygen species reported by ex-situ or quasi in situ methods could be attributed to the rapid re-oxidation of OD-Cu, which is due to the high reactivity of numerous surface grain boundaries exposed to ambient air or moist environment. Therefore, it is underlining that the investigation of subsurface oxygen should be conducted in a carefully designed experimental condition since a correct description of the OD-Cu surface region is crucial to faithfully determine a reaction mechanism.

Hard X-ray photoelectron spectroscopy (HAXPES) with high-grazing incident light was employed to probe the existence of subsurface oxygen in OD-Cu with non-destructive depth profiling. Photoelectron spectroscopy is commonly employed to probe chemical shifts of the same element in different environments. Especially, hard X-rays permits deeper probing into the bulk of materials than what soft X-rays do while the high-grazing incidence angle also permits being surface sensitive. To achieve the depth profiling in this study,

[*] H.-Y. Wang,[+] M. Soldemo,[+] D. Degerman, P. Lömker, A. Nilsson, P. Amann
Department of Physics, AlbaNova University Center
Stockholm University, 10691 Stockholm (Sweden)
E-mail: wang.hy@fysik.su.se
P. Lömker, C. Schlueter
Photon Science, Deutsches Elektronen-Synchrotron (DESY)
22607 Hamburg (Germany)
P. Amann
Current address: Scienta Omicron AB
Danmarksgatan 22, 75323 Uppsala (Sweden)
[+] These authors contributed equally to this work.
Supporting information and the ORCID identification number(s) for the author(s) of this article can be found under: https://doi.org/10.1002/anie.202111021.

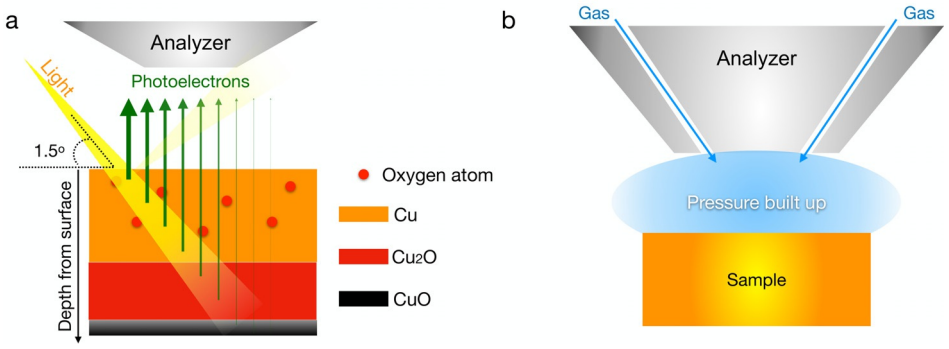

Figure 1. Illustration of the experiment. a) Top view of XPS measurements with grazing incidence of light and normal emission of photoelectrons, where the analyzer is placed in the horizontal direction and photoelectrons are induced from different depths. The widths of the photoelectron arrows illustrate different attenuation effects, where thinner arrow coming from deeper layers gives less contribution to acquired spectra. b) Oxidation or reduction of sample in the vacuum chamber by guiding the desired gases onto the sample surface through the special front cone design.

the high-grazing incidence angle of light was kept fixed while varying the photon energy, increased photon energy leads to increased probing depth. The probing depth is not only determined by the X-ray attenuation length within the material but mainly dominated by the photoelectron inelastic mean-free path (IMFP), illustrated schematically in Figure 1a, where atoms deeper beneath the surface contributes weaker to the spectra than those closer to the surface. The probing depth is usually defined as $3\times$IMFP of the photoelectrons, which corresponds to roughly 95% of the integrated signal, assuming a uniform distribution. For this study, however, the amounts of subsurface oxygen is low and hence to account for the signal-to-noise ratio, the probing depth is here redefined as 90% of the integrated signal, which is usually interpreted as the information depth. (see the Supporting Information for estimations of probing depths used). The experiment was conducted using POLARIS instrument situated at beamline P22 of Petra III at DESY in Hamburg, Germany.[12] The P22 beamline is capable to provide hard X-rays between 3.0 to 10.0 keV and the experimental geometry was set to a light incidence angle of 1.5° with respect to the surface and normal emission of photoelectrons, as illustrated in Figure 1a. The POLARIS instrument is designed for operating under elevated gas pressures and can expose the sample surface to gases from the electron analyzer's front cone, see illustration in Figure 1b. Since OD-Cu can be synthesized by either electrochemical reduction or by thermal H_2 reduction of the Cu oxide precursors, the H_2 reduction method was adopted here as it is straight forward implementable in the vacuum chamber environment. Since no sample transfer is being made between the H_2 reduction step and the data acquisition, no exposure to the ambient atmosphere is needed, which would have contaminated the sample's surface. The preparation of OD-Cu followed the method reported by Arnau et al.[13] In short, the Cu oxide precursor was produced by calcination of a piece of polycrystalline Cu specimen with air in a muffle furnace and subsequently subjected into POLARIS chamber for H_2 reduction at a pressure of 300 mbar and a temperature of 140 °C (see detailed experimental procedure in supplementary information). In addition, to facilitate the data interpretation, a Cu_2O reference surface was prepared by oxidation of the Cu specimen right in front of the electron analyzer to collect reference signals. During the measurements, the specimen was kept at 140 °C in high-vacuum environment to minimize the risk of trace gases adsorbing onto the surface that could obscure the results. The present study aims to establish a high-resolution spectral feature of subsurface oxygen and potentially distinguish the unique interaction between subsurface oxygen, oxides and Cu metal after exposure to a strong reducing environment.

Results and Discussion

After air calcination of the polycrystalline Cu specimen, the as-prepared Cu oxide precursor exhibits a dark and rough appearance (Figure S1a), which is the typical color of cupric oxide (CuO).[14] The electrically insulating characteristics of a thick CuO layer resulted in extensive charge build-up making XPS studies unfeasible. After the H_2 reduction treatment, the OD-Cu exhibits a shining orange/pink color (see Figure S1b), indicating the oxide has been reduced across the entire sample surface.[14] A representative XPS survey spectrum of the OD-Cu recorded using 3266 eV photons is shown in Figure S2, depicting presence of copper and oxygen without detectable traces of the common contaminants from the ambient heat treatment or from the vacuum chamber, for example, S, Si, and C. Figure S3 shows the XPS Cu 2p region of OD-Cu probed with multiple different photon energies for depth profiling and Cu_2O (reference sample prepared separately), where its two spin-orbit split components feature at 932.8 eV for $2p_{3/2}$ and 952.6 eV for $2p_{1/2}$ can be clearly seen. In addition to the spin-orbit split components, the Cu_2O reference sample also shows two additional weak satellites between the two spin-orbit split peaks. Unfortunately, the overlap in binding energy for the Cu 2p spin-orbit components of metallic Cu (Cu^0) and Cu_2O (Cu^I) makes it notoriously difficult to separate the respective contribution and quantify relative contribution.[15] It is, however, still possible to rule out contribution from CuO (Cu^{II}) in the surface region due to the fact it shows a higher binding energy of spin-orbit components and significant satellite features.[15]

To unambiguously elucidate the oxidation state of the copper in OD-Cu, the Auger electron decay of $L_3M_{4,5}M_{4,5}$ is resorted as shown in Figure 2a. The principal peak in Cu LMM is shifted by 1.9 eV between Cu_2O and metallic Cu,[15,16] enabling the discrimination between them. As the kinetic energies of Auger electrons depend on the decay processes rather than the photon energy of the core-hole creating X-ray

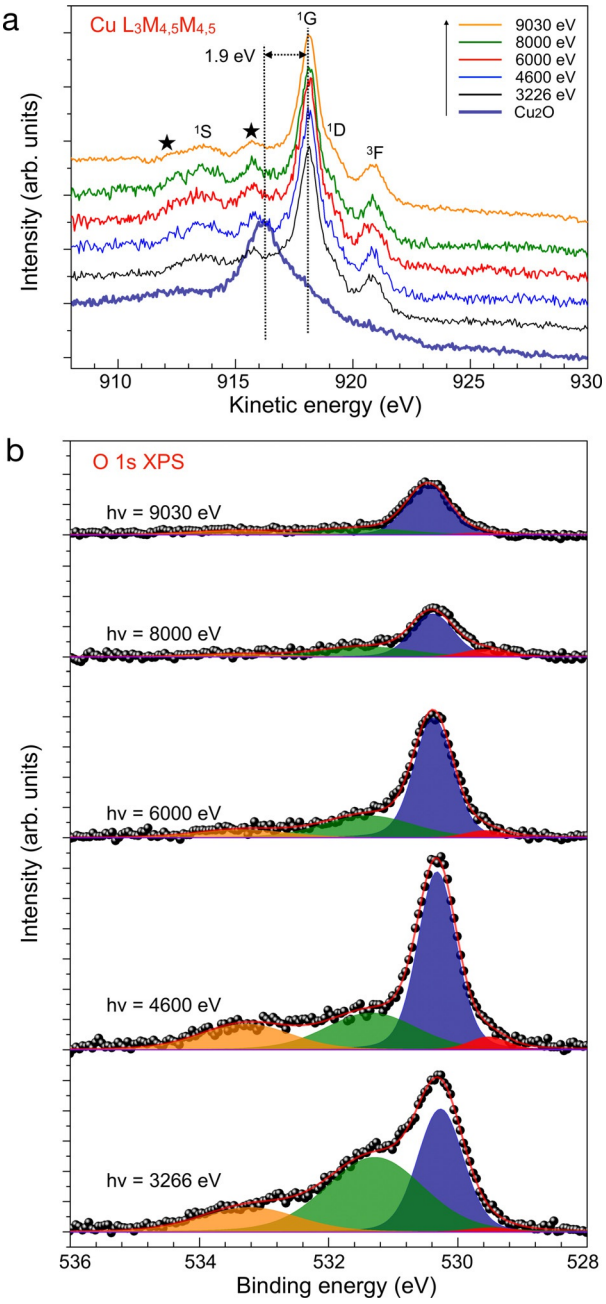

Figure 2. a) The Augur spectra of Cu $L_{2,3}M_{4,5}M_{4,5}$ probed with various photon energies. The Auger process of Cu^0 results in $3d^8$ electronic configuration and because of the LS-coupling the final-state term is splitting into 5 components,[16] namely ^3F, ^1D, ^3P, ^1G and ^1S except ^3P due to its low intensity. Two extra intensities marked with stars are also observed, which are attributed to $L_2L_3M_{4,5}$ Coster–Kronig effect.[19] The Cu_2O reference spectra were all recoded using 9030 eV photon energy. b) The peak-fitting results of O1s XPS spectra where the Shirley background has been subtracted. Red: CuO, Blue: Cu_2O, green: $O_{Cu,vac}$, and orange: O_{int}.

photons, the IMFP of the Auger Cu LMM electrons is actually the limiting factor for the probing depth even for the hard X-ray measurement. The dominating state of copper in the surface near region down to 33 Å (the estimated information depth of Auger Cu LMM electrons, see supplementary information) is determined to be metallic.[15] Importantly, these results can confidently exclude the significant existence of Cu_2O, CuO, or $Cu(OH)_2$ at the near-surface region, which could potentially be formed on the surface during OD-Cu formation. A study using DFT calculations has suggested that CO_2RR products should only form on the metallic Cu surface since the reduction of Cu oxide is kinetically and energetically more favorable than CO_2RR.[17] In addition, in situ grazing incidence X-ray absorption spectroscopy and X-ray diffraction studies have suggested no existence of Cu_2O at the surface after electrochemical reduction.[18] The spectra in Figure 2a are in good agreement with all these results.

In contrast to the Auger Cu LMM measurements, the kinetic energy of the photoelectrons in XPS are directly photon energy dependent. This means the photoelectron IMFP significantly changes with photon energy and hence also the probing depth. XPS spectra of the O 1s region measured using the same photon energies as for Auger Cu LMM are shown in Figure S4. They are presented as normalized to the height of the strongest peak to visualize the spectral structural changes. The dominating feature for all photon energies is located at around 530.3 eV and the relative intensities of the other components get smaller with increasing photon energy, that is, probing depth, suggesting the contribution of the other species are closer to the surface. The binding energy of this dominating feature corresponds well to Cu_2O but not to CuO.[20] The growth in relative intensity of Cu_2O contribution with increasing probing depth adds weight to the interpretation that the Cu_2O is mainly buried beneath the reduced copper layer rather than being present in the surface region. The presence of atomic oxygen on the copper surface can also be ruled out since that usually appears at around 529.8 eV.[21] It should be noted that the additional contribution on the Cu_2O component's low binding energy side appears at increasing photon energies, which means it is physically located deeper into the bulk and should origin from CuO, where the details will be discussed later. On the high binding energy side next to the Cu_2O peak, from ca. 531 to ca. 535 eV, there is a continuous spectral structure with obvious multiple components. Remembering that the spectra were recorded while the sample temperature was held at 140 °C, the most common surface oxygen containing contaminants, such as H_2O, -OH, and O_2, can be excluded since they are bonding too weakly to metallic Cu in order to produce the observed intensity.[22] It should be kept in mind that these aforementioned species are still possibly reside at the surface, but due to the fact that the experiment using high photon energy up to 9030 eV, the contribution from a low surface coverage to the signal is negligible. Hence, the observed signal on the high-binding energy side cannot be explained by the commonly expected sources of spectral contribution in this region. Also, the XPS C 1s region was clean (see Figure S2), meaning no organic or other carbon containing compounds were detected. Moreover, studying the intensity development of the high binding energy components relative to the Cu_2O component as function of photon energy strongly suggests these oxygen species are located between the OD-Cu's surface and the buried Cu_2O layer.

To obtain a better understanding of how the relative intensities of the components develop with increased probing

depth and to assign the contributions to different kinds of oxygen species, peak fitting of the XPS O 1s region was carried out as shown in Figure 2b, see the supplementary information for peak fitting details. Following from visual inspection of the spectral shape in Figure S4, it is apparent that two components are needed to accurately describe the changes in spectral shape changes on the high-binding energy side of the Cu_2O peak at the different photon energies. The structure in OD-Cu has been reported to contain a huge amount of structural defect sites by positron annihilation spectroscopy (PAS).[9] DFT studies of the copper lattice upon Cu_2O reduction has been reported to be heavily distorted.[8b] Thus, for each kind of oxygen species present inside the OD-Cu structure, there will be a distribution of many similar but slightly different sites, each having slightly different binding energy. This together with a higher chance to coordinate with more Cu atoms[23] as the oxygen is embedded in the Cu structure will give rise to significant peak broadening relative what would been expected in a perfect crystalline specimen where the contribution to each component would origin from one specific site. For these reasons, the components for the peak deconvolution of the O1s region will feature a large full-width half-maximum (FWHM).

The peak deconvolution of the XPS O 1s-region in Figure 2b shows that four components are needed to accurately provide a description on the spectral shape development as function of photon energy. The main peak is Cu_2O and the low binding energy tail is assigned to CuO. The CuO tail gets significant for the high photon energy measurement, where the estimated probing depth for 8000 eV is 185 Å. The relative CuO contribution grows with probing depth, meaning it either is incorporated as non-reduced patches in the Cu_2O region or is situated beneath the Cu_2O region, which would follow from the reduction of the starting CuO to OD-Cu. The two high binding energy components, centered at 531.3 eV and 533.2 eV, respectively, are suggested to origin within the metallic copper layer due to how their relative intensities change with varying the photon energy. Although a direct observation of the interaction of subsurface oxygen with neighboring Cu atoms inside the bulk is difficult, studies of adsorbed oxygen over metallic Cu surface (denoted as O/Cu)[23] may provide useful insight. For oxygen atoms adsorbed on reconstructed copper, mild shake-up features at higher binding energy of around 533 eV for a main component at 529.5 eV has been reported. This shake-up feature is ascribed to the intrinsic process occurring around the ionized adsorbed oxygen atom in local O/Cu electronic structure during the photoionization process, where the similar behavior has been discussed in the studies of C, N, or O adsorbed on other metal surfaces as well.[24] It should be mentioned that this is not the case for the oxygen in an oxide phase, where the lattice oxygen is an anion and covalently shares electrons with the formally closed d-shell Cu cations in Cu_2O. Furthermore, these spectral features do not scale equally with changing probing depth, meaning their origins are not correlated. Hence, the two high-binding energy components are not shake-up features of the main peak of Cu_2O and nor is the 533.2 eV component a shake-up to the 531.3 eV component.

During the preparation of OD-Cu, the oxygen from the bulk oxide need to diffuse through the reduced copper to the surface. In oxygen diffusion models for copper, two distinctly different kinds of oxygen species have been proposed: (i) oxygen in copper vacancy sites or lattice defects ($O_{Cu,vac}$) and (ii) interstitial oxygen (O_{int}).[25] Both kinds of subsurface oxygen are illustrated in Figure 3a. Oxygen atoms accommodating at lattice vacancy sites in perovskites have been reported at a binding energy of ca. 531.4 eV,[26] coinciding well with the component found in our spectra at ca. 531.3 eV. Furthermore, oxygen species residing at lattice metal vacancies have also been reported in metal oxides.[27] This binding energy position is also in line with the previous in situ XPS study, where the formation of subsurface oxygen species after CO_2RR was proposed at the binding energy of 531.7 eV and a computed binding energy position relative to the chemisorbed oxygen support this suggestion.[28] Therefore, we propose the component at 531.3 eV can be assigned to the subsurface oxygen occupying at lattice defect and/or Cu vacancy sites ($O_{Cu,vac}$). Interstitial oxygen species, centered at around 533 eV, has also been widely reported in ZnO system,[29] and the similarity of d band electronic structure of Zn and Cu (d^{10} in both cases) rationalizes the analogous peak position of O_{int} trapped in metallic Cu. The O_{int} atoms reside very close to the center between Cu atoms and can easily rotate around a Cu-Cu bond, leading to a strain in the Cu lattice and a high binding energy position of due to its similarity to free oxygen atoms. Therefore, the 533.2 eV component is assigned to interstitial oxygen in the reduced disordered metallic copper layer (O_{int}).

Figure 3b shows the relative intensities for the different oxygen species for the different photon energies as obtained from the peak fitting shown in Figure 2b. It shows that at the most surface sensitive probing (photon energy of 3266 eV), the $O_{Cu,vac}$ is significantly stronger than O_{int}, but such difference is effectively vanished when probing with 4600 eV photons. This observation indicates that $O_{Cu,vac}$ species is significantly more present at the near-surface region (estimated here to about the first 5–10 atomic layers beneath the surface as the intensity contribution is exponentially decaying with depth from the surface and this region contributes less to the total spectrum with increasing photon energy, than O_{int}), which is in agreement with studies.[10] It suggests that the interstitial oxygen is not stable in the near-surface region of copper. During the reduction process, the metallic copper lattice which is gradually formed on top of Cu_2O, will be defect rich and the copper atoms will not order in a perfect face-centered cubic lattice structure, as calculated by Chiang et al.[8b] As a consequence, the defect/ vacancy rich copper film would permit $O_{Cu,vac}$ to stay even in the near-surface region. As the dissolved oxygen atoms, predominantly in form of O_{int} (the diffusion rate is reported to be significantly larger for O_{int} than for $O_{Cu,vac}$[25]), diffuse from the buried Cu_2O layer to the surface through the defect/vacancy rich copper layer during the reduction process, this means $O_{Cu,vac}$ can tentatively be formed when an O_{int} interact with a such copper vacancy/ defect site. The $O_{Cu,vac}$ could also be formed at defects in the copper film at the OD-Cu/Cu_2O interface directly upon

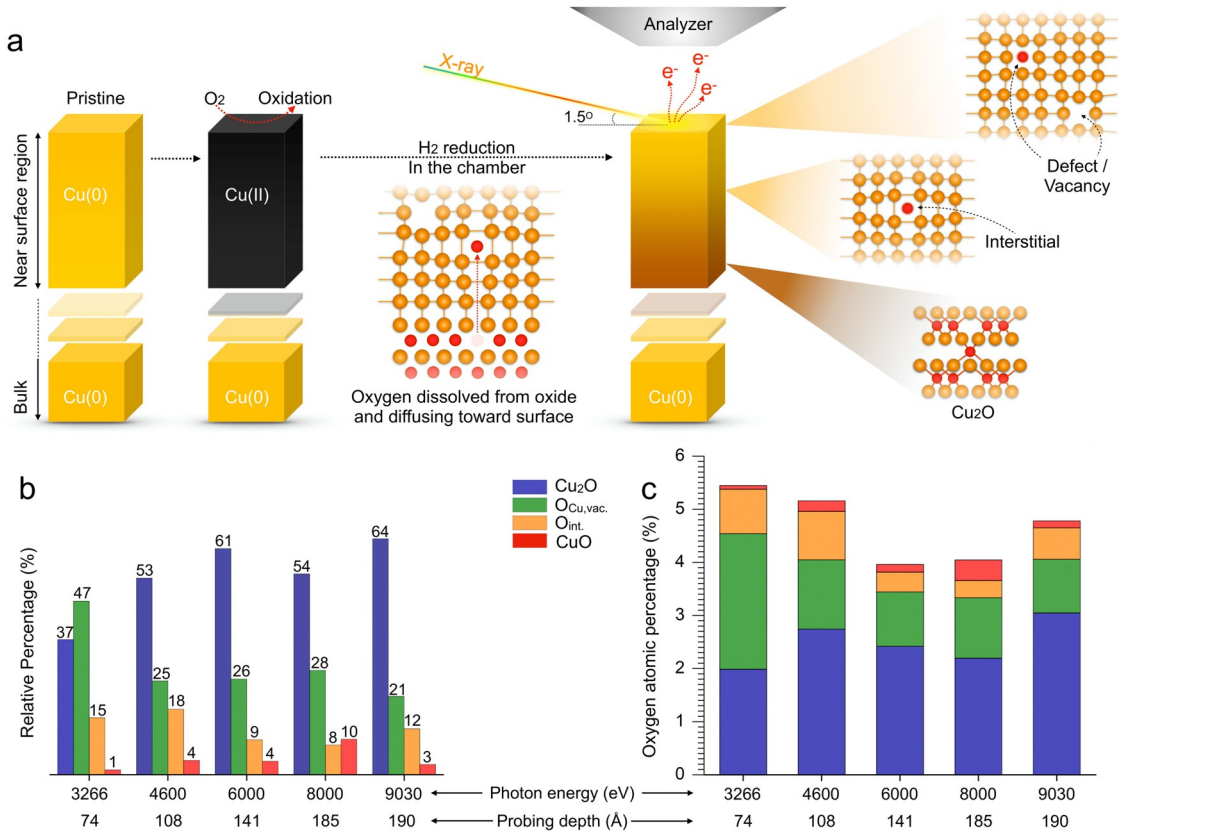

Figure 3. a) The illustration of two different subsurface oxygen species, $O_{Cu,vac.}$ and $O_{int.}$, formation during OD-Cu preparation, where a defect/vacancy rich surface is generated by Cu atom rearrangement under H_2 treatment in the chamber, and the lattice oxygen is dissolved from the oxide and then diffuses toward the surface as $O_{int.}$ b) The relative percentage between different oxygen containing species, and c) oxygen atomic percentage in the material, where the summation of total oxygen containing species and Cu is 100%, probed with different photon energies in terms of probing depths. The probing depth is estimated of reaching 90% of the total integrated signal based on the photoelectrons emitted from O 1s core-level (see the Supporting Information for the calculation).

reduction rather than requiring oxygen atoms diffuse through the metallic copper film.

The constructed model, based on the spectroscopy data, tells there is a Cu_2O layer buried underneath a reduced copper film. This is understood from the relative intensity changes of the deconvoluted components in XPS O 1s as a function of photon energy and the dominating metallic copper signal in Auger Cu LMM. In literature,[30] Cu_2O has been frequently reported to appear under operando CO_2RR conditions by probing with a bulk sensitive technique. A misinterpretation that this Cu_2O would to a significant extent be present at the surface or close to the surface may lead towards an erroneous determination of the reaction mechanisms as the oxide if buried shallowly has an impact on the surface properties. Herein, our spectroscopy data shows a change in the intensity ratio for the subsurface oxygen species with increased probing depth which strongly suggests the presence of subsurface oxygen in form of $O_{Cu,vac}$ within the atomic layers just beneath the surface of the metallic copper. A recent theory work has pointed out a disordered metallic Cu surface with subsurface oxygen species underneath is the essential combination for forming organic products from CO_2RR.[31] It is noteworthy that the high binding energy of $O_{Cu,vac}$ is believed to be the unique characteristic of electrophilic oxygen atoms bounded to crystal defective sites and is not indicative of molecular species.[32] The presence of the electrophilic oxygen atoms, $O_{Cu,vac}$, underneath the metallic Cu surface imply a complex interaction with Cu. This interlinkage is further proposed to reduce the σ-repulsion by withdrawing electron density from the Cu sp-band, resulting in a net enhancement of the binding energy of the key CO intermediates on the Cu surface during CO_2RR.[8b,c] The O_{int} species is here thought of the oxygen dissolved from Cu oxide during reduction that upon interaction with copper lattice vacancy sites may form $O_{Cu,vac}$. If the O_{int} diffuses through the metallic copper and reaches the top-most atomic layers, it will be reacted away by the reducing environment.

Owing to fact that the H_2 reduction process occurring is starting from the surface, it is expected that the remaining Cu_2O is within the bulk yet the Cu/Cu_2O interface moves deeper away from the surface with reduction treatment processing, which is manifested by the increasing Cu_2O relative intensity with the increasing X-ray photon energy. The ratio of the integrated intensity of all oxygen species in O 1s ($O_{Cu,vac}$, O_{int}, Cu_2O, and CuO) and the relative copper intensity based on Cu $2p_{3/2}$ for each photon energy, normalized to photoionization cross-section and signal attenuation, is estimated as shown in Figure 3c. The trend of such O-to-Cu

ratio changes with probing depth could be comprehended as following: the decrease of oxygen concentration percentage from around 5.4 to 4.0 % is majorly due to the deeper probing that includes more Cu signal. Combining the information from both Figure 3b and Figure 3c, we can estimate the real qualitative concentration distribution of each oxygen species as function of incident photon energy (shown in the supplementary information). The increase in oxygen concentration when further increasing the photon energy up to 9030 eV could be ascribed to the shorter X-ray attenuation length caused by Cu 1s absorption edge (8979 eV). The shorter X-ray attenuation length also explains the decrease of the CuO component as the CuO is buried deeper. It should also be kept in mind that the signal-to-noise ratio is decreasing with higher photon energy, which makes the determination of relative intensity of the subsurface oxygen species less accurate and more ambiguous. The interpretation shall be qualitative trends rather than quantitative changes.

Conclusion

OD-Cu has been studied using non-destructive depth profiling by the means of grazing incident hard X-ray photoelectron spectroscopy and Auger electron spectroscopy. The depth profiling of the OD-Cu specimen reveals a metallic top layer and a buried oxide beneath. The shallow probing of Auger Cu LMM rules out the presence of oxide at the surface. This allows us to conceive the system post reduction, which further reveals two different kinds of subsurface oxygen species in OD-Cu: (i) $O_{Cu,vac}$ binding to copper vacancies and defects in the copper lattice and is the dominating subsurface oxygen species in the near surface region, and (ii) O_{int} being beneath the top copper atomic layers and only in insignificant amount in near surface region. The buried oxide underneath comprises of Cu_2O as main species and CuO as minority species. The CuO species is suggested to be situated beneath the Cu_2O layer as its contribution grows with increased probing depth and is barely observed for the shallower probing. The spectral features of $O_{Cu,vac}$ induced by the interaction to metallic Cu suggest that $O_{Cu,vac}$ possesses the potential impact toward Cu surface chemistry for boosting CO_2RR. Maintaining a high concentration of subsurface oxygen by, e.g., oxygen plasma treatment[33] or periodically oxidizing and reducing the Cu surface[34] could be the strategies to alter the electrocatalytic performance. Together with our previous electrochemical experiments[9,28] and simulation works,[8b,c] the presented data completes the story and provides a clear picture regarding the detailed composition at the near-surface region of OD-Cu. Furthermore, our spectral results suggest that no significant amounts of Cu_2O is present at the surface level under reducing condition, which is rather important for a correct interpretation of surface reaction dynamics of CO_2RR.

Acknowledgements

This work was supported by the Swedish Research Council under Grant No 2013–8823, the Knut & Alice Wallenberg (KAW) foundation under Grant No 2016.0042 as well as the Swedish Foundation for strategic research (Stiftelsen för Strategisk Forskning, SSF), proj. Nr. ITM 17-0034. We acknowledge DESY (Hamburg, Germany), a member of the Helmholtz Association HGF, for the provision of experimental facilities, and this research was carried out at PETRA. Beamtime was allocated for proposal II-20190003 EC.

Conflict of Interest

The authors declare no conflict of interest.

Keywords: CO_2 reduction · grazing incident XPS · oxide-derived Cu · subsurface oxygen · surface-sensitive measurement

[1] Y. Y. Birdja, E. Perez-Gallent, M. C. Figueiredo, A. J. Gottle, F. Calle-Vallejo, M. T. M. Koper, *Nat. Energy* **2019**, *4*, 732 – 745.
[2] a) Y. Hori, H. Wakebe, T. Tsukamoto, O. Koga, *Electrochim. Acta* **1994**, *39*, 1833 – 1839; b) Y. Hori, K. Kikuchi, S. Suzuki, *Chem. Lett.* **1985**, *14*, 1695 – 1698.
[3] a) C. W. Li, M. W. Kanan, *J. Am. Chem. Soc.* **2012**, *134*, 7231 – 7234; b) C. W. Li, J. Ciston, M. W. Kanan, *Nature* **2014**, *508*, 504 – 507; c) F. S. Roberts, K. P. Kuhl, A. Nilsson, *Angew. Chem. Int. Ed.* **2015**, *54*, 5179 – 5182; *Angew. Chem.* **2015**, *127*, 5268 – 5271; d) A. Eilert, F. S. Roberts, D. Friebel, A. Nilsson, *J. Phys. Chem. Lett.* **2016**, *7*, 1466 – 1470.
[4] a) A. S. Hall, Y. Yoon, A. Wuttig, Y. Surendranath, *J. Am. Chem. Soc.* **2015**, *137*, 14834 – 14837; b) A. S. Varela, M. Kroschel, T. Reier, P. Strasser, *Catal. Today* **2016**, *260*, 8 – 13; c) F. S. Roberts, K. P. Kuhl, A. Nilsson, *ChemCatChem* **2016**, *8*, 1119 – 1124.
[5] X. F. Feng, K. L. Jiang, S. S. Fan, M. W. Kanan, *ACS Cent. Sci.* **2016**, *2*, 169 – 174.
[6] H. Xiao, W. A. Goddard, T. Cheng, Y. Y. Liu, *Proc. Natl. Acad. Sci. USA* **2017**, *114*, 6685 – 6688.
[7] M. Favaro, H. Xiao, T. Cheng, W. A. Goddard, J. Yano, E. J. Crumlin, *Proc. Natl. Acad. Sci. USA* **2017**, *114*, 6706 – 6711.
[8] a) W. Zhang, C. Q. Huang, Q. Xiao, L. Yu, L. Shuai, P. F. An, J. Zhang, M. Qiu, Z. F. Ren, Y. Yu, *J. Am. Chem. Soc.* **2020**, *142*, 11417 – 11427; b) C. Liu, M. P. Lourenco, S. Hedstrom, F. Cavalca, O. Diaz-Morales, H. A. Duarte, A. Nilsson, L. G. M. Pettersson, *J. Phys. Chem. C* **2017**, *121*, 25010 – 25017; c) C. Liu, S. Hedstrom, J. H. Stenlid, L. G. M. Pettersson, *J. Phys. Chem. C* **2019**, *123*, 4961 – 4968.
[9] F. Cavalca, R. Ferragut, S. Aghion, A. Eilert, O. Diaz-Morales, C. Liu, A. L. Koh, T. W. Hansen, L. G. M. Pettersson, A. Nilsson, *J. Phys. Chem. C* **2017**, *121*, 25003 – 25009.
[10] a) A. J. Garza, A. T. Bell, M. Head-Gordon, *J. Phys. Chem. Lett.* **2018**, *9*, 601 – 606; b) M. Fields, X. Hong, J. K. Norskov, K. Chan, *J. Phys. Chem. C* **2018**, *122*, 16209 – 16215.
[11] Y. W. Lum, J. W. Ager, *Angew. Chem. Int. Ed.* **2018**, *57*, 551 – 554; *Angew. Chem.* **2018**, *130*, 560 – 563.
[12] a) C. Schlueter, A. Gloskovskii, K. Ederer, S. Piec, M. Sing, R. Claessen, C. Wiemann, C. M. Schneider, K. Medjanik, G. Schönhense, P. Amann, A. Nilsson, W. Drube, *Synchrotron Radiat. News* **2018**, *31*, 29 – 35; b) P. Amann, D. Degerman, M. T. Lee, J. D. Alexander, M. Shipilin, H.-Y. Wang, F. Cavalca, M.

Weston, J. Gladh, M. Blom, M. Bjorkhage, P. Lofgren, C. Schlueter, P. Loemker, K. Ederer, W. Drube, H. Noei, J. Zehetner, H. Wentzel, J. Ahlund, A. Nilsson, *Rev. Sci. Instrum.* **2019**, *90*, 103102.
[13] A. Verdaguer-Casadevall, C. W. Li, T. P. Johansson, S. B. Scott, J. T. McKeown, M. Kumar, I. E. L. Stephens, M. W. Kanan, I. Chorkendorff, *J. Am. Chem. Soc.* **2015**, *137*, 9808 – 9811.
[14] J. Zhang, H. W. Richardson, in *Ullmann's Encyclopedia of Industrial Chemistry*, Wiley-VCH, Weinheim, **2016**, pp. 1 – 31.
[15] M. C. Biesinger, *Surf. Interface Anal.* **2017**, *49*, 1325 – 1334.
[16] N. Pauly, S. Tougaard, F. Yubero, *Surf. Sci.* **2014**, *630*, 294 – 299.
[17] L. Mandal, K. R. Yang, M. R. Motapothula, D. Ren, P. Lobaccaro, A. Patra, M. Sherburne, V. S. Batista, B. S. Yeo, J. W. Ager, J. Martin, T. Venkatesan, *ACS Appl. Mater. Interfaces* **2018**, *10*, 8574 – 8584.
[18] S. H. Lee, J. C. Lin, M. Farmand, A. T. Landers, J. T. Feaster, J. E. A. Acosta, J. W. Beeman, Y. F. Ye, J. Yano, A. Mehta, R. C. Davis, T. F. Jaramillo, C. Hahn, W. S. Drisdell, *J. Am. Chem. Soc.* **2021**, *143*, 588 – 592.
[19] P. Weightman, P. T. Andrews, *J. Phys. C* **1979**, *12*, 943 – 957.
[20] J. A. Anderson, J. L. G. Fierro, *J. Solid State Chem.* **1994**, *108*, 305 – 313.
[21] K. Andersson, G. Ketteler, H. Bluhm, S. Yamamoto, H. Ogasawara, L. G. M. Pettersson, M. Salmeron, A. Nilsson, *J. Phys. Chem. C* **2007**, *111*, 14493 – 14499.
[22] K. Andersson, G. Ketteler, H. Bluhm, S. Yamamoto, H. Ogasawara, L. G. M. Pettersson, M. Salmeron, A. Nilsson, *J. Am. Chem. Soc.* **2008**, *130*, 2793 – 2797.
[23] H. Tillborg, A. Nilsson, B. Hernnas, N. Martensson, *Surf. Sci.* **1992**, *269*, 300 – 304.
[24] A. Nilsson, N. Martensson, *Chem. Phys. Lett.* **1991**, *182*, 147 – 151.
[25] H. Magnuson, K. Frisk, in *Rapport/ Institutet för metallforskning*, Swerea KIMAB AB, **2014**, pp. 1 – 39.
[26] N. Yamazoe, Y. Teraoka, T. Seiyama, *Chem. Lett.* **1981**, *10*, 1767 – 1770.
[27] a) X. H. Lu, Y. X. Zeng, M. H. Yu, T. Zhai, C. L. Liang, S. L. Xie, M. S. Balogun, Y. X. Tong, *Adv. Mater.* **2014**, *26*, 3148 – 3155; b) J. C. C. Fan, J. B. Goodenough, *J. Appl. Phys.* **1977**, *48*, 3524 – 3531.
[28] A. Eilert, F. Cavalca, F. S. Roberts, J. Osterwalder, C. Liu, M. Favaro, E. J. Crumlin, H. Ogasawara, D. Friebel, L. G. M. Pettersson, A. Nilsson, *J. Phys. Chem. Lett.* **2017**, *8*, 285 – 290.
[29] a) R. Saha, N. R. Saha, A. Karmakar, G. K. Dalapati, S. Chattopadhyay, *J. Mater. Sci. Mater. Electron.* **2019**, *30*, 8796 – 8804; b) H. B. Fan, S. Y. Yang, P. F. Zhang, H. Y. Wei, X. L. Liu, C. M. Jiao, Q. S. Zhu, Y. H. Chen, Z. G. Wang, *Chin. Phys. Lett.* **2007**, *24*, 2108 – 2111.
[30] T. C. Chou, C. C. Chang, H. L. Yu, W. Y. Yu, C. L. Dong, J. J. Velasco-Velez, C. H. Chuang, L. C. Chen, J. F. Lee, J. M. Chen, H. L. Wu, *J. Am. Chem. Soc.* **2020**, *142*, 2857 – 2867.
[31] G. Liu, M. Lee, S. Kwon, G. Zeng, J. Eichhorn, A. K. Buckley, F. D. Toste, W. A. Goddard, F. M. Toma, *Proc. Natl. Acad. Sci. USA* **2021**, *118*, e2012649118.
[32] M. Salmeron, R. Schlögl, *Surf. Sci. Rep.* **2008**, *63*, 169 – 199.
[33] H. Mistry, A. S. Varela, C. S. Bonifacio, I. Zegkinoglou, I. Sinev, Y. W. Choi, K. Kisslinger, E. A. Stach, J. C. Yang, P. Strasser, B. Roldan Cuenya, *Nat. Commun.* **2016**, *7*, 12123.
[34] R. M. Arán-Ais, F. Scholten, S. Kunze, R. Rizo, B. Roldan Cuenya, *Nat. Energy* **2020**, *5*, 317 – 325.

Manuscript received: August 16, 2021
Revised manuscript received: October 19, 2021
Accepted manuscript online: November 10, 2021
Version of record online: December 10, 2021